Changes in Tornado Climatology Accompanying the Enhanced Fujita Scale

ROGER EDWARDS,[a] HAROLD E. BROOKS,[b] AND HANNAH COHN[c,d]

[a] *Storm Prediction Center, National Weather Service, Norman, Oklahoma*
[b] *National Severe Storms Laboratory and School of Meteorology, University of Oklahoma, Norman, Oklahoma*
[c] *IBM Weather Company, Dallas, Texas*
[d] *American Airlines, Dallas, Texas*

(Manuscript received 30 March 2021, in final form 23 August 2021)

ABSTRACT: U.S. tornado records form the basis for a variety of meteorological, climatological, and disaster-risk analyses, but how reliable are they in light of changing standards for rating, as with the 2007 transition of Fujita (F) to enhanced Fujita (EF) damage scales? To what extent are recorded tornado metrics subject to such influences that may be nonmeteorological in nature? While addressing these questions with utmost thoroughness is too large of a task for any one study, and may not be possible given the many variables and uncertainties involved, some variables that are recorded in large samples are ripe for new examination. We assess basic tornado-path characteristics—damage rating, length, width, and occurrence time, as well as some combined and derived measures—for a 24-yr period of constant path-width recording standard that also coincides with National Weather Service modernization and the WSR-88D deployment era. The middle of that period (in both time and approximate tornado counts) crosses the official switch from F to EF. At least minor shifts in all assessed path variables are associated directly with that change, contrary to the intent of EF implementation. Major and essentially stepwise expansion of tornadic path widths occurred immediately upon EF usage, and widths have expanded still farther within the EF era. We also document lesser increases in pathlengths and in tornadoes rated at least EF1 in comparison with EF0. These apparently secular changes in the tornado data can impact research dependent on bulk tornado-path characteristics and damage-assessment results.

KEYWORDS: Atmosphere; North America; Severe storms; Tornadoes; Data quality control; Damage assessment

1. Background

United States tornado data are gathered by local National Weather Service (NWS) offices, compiled in county-segmented form by NCEI (formerly NCDC), and then molded into whole-path "One Tornado" (ONETOR) files made freely available by the Storm Prediction Center (Schaefer and Edwards 1999; https://www.spc.noaa.gov/wcm/#data). Path characteristics in ONETOR include start and end times, starting and ending locations (via state, latitude, and longitude), pathlengths and widths, nonagricultural and crop damage codes corresponding to ranges of dollar values, direct deaths and injuries, and damage ratings based on the maximum damage indicator (DI) found in each path. Tornadoes in ONETOR were observed directly by eyewitnesses, were inferred from remote sensing (such as radar imagery) that motivated subsequent survey-based verification, or were discovered post facto from otherwise surveyed damage patterns (Schaefer and Edwards 1999; Edwards et al. 2013).

While true intensity of tornadoes cannot be known, nor sampled directly along an entire path, tornado strength has been inferred through peak-DI damage intensity according to two successive measures: the Fujita (F) scale (e.g., Fujita 1971, 1981), applied to tornado records from 1950 through January 2007, and the enhanced Fujita (EF) scale (Wind Science and Engineering Center 2006), implemented in February 2007 (LaDue and Ortega 2008). These scales differ considerably from each other in terms of precision and application, leading to our general motivating hypothesis for this work: that the switch from F to EF brought about climatologically apparent changes in recorded tornado characteristics.

Final tornado ratings in both scales are based on the maximum known damage point of each tornado, on a six-step scale numbered from 0 to 5, representing weakest to strongest damage as the number increases. Submaximal DIs also are rated along most paths, to estimate point ranges of the fastest quarter-mile (0.4 km) of responsible wind (McDonald 2001; Edwards et al. 2013). The NWS adopted the F scale for official rating purposes in a gradual process during the mid-1970s. This included retroactively rating tornadoes to 1950, based largely on photographs, printed news accounts, and descriptions available in NCDC *Storm Data* periodicals. For that retroactive-rating era, Agee and Childs (2014) documented apparent secular enhancement of F2 ratings, at the expense of F1. This relative F2 enhancement also was apparent in the earlier work of Verbout et al. (2006), although it was not identified specifically as the retroactive-rating era. To segregate generally weaker, less-impactful events from the most deadly and damaging ones, for research and forecasting applications, Hales (1988) introduced the notion of significant (F2–F5) tornadoes, a practice that became well established in tornado climatology during the remainder of the F era (e.g., Grazulis 1993), and has remained customary for the corresponding EF levels in research and operations [e.g., herein, and with explicit significant-tornado forecasts in SPC outlooks, per Edwards et al. (2015)].

The F scale nominally was based on "well built" houses; however, damages to both other human structures and vegetation,

Corresponding author: Roger Edwards, roger.edwards@noaa.gov

DOI: 10.1175/JAMC-D-21-0058.1

such as crops and trees, often were used to infer wind speeds and assign corresponding F ratings (e.g., Wurman and Alexander 2005), including by the inventor of the scale (e.g., Fujita 1989, 1992, 1993). Leading up to and motivating EF-scale development, concerns grew among wind engineers and research and operational meteorologists about the F scale's subjectivity, imprecision, inconsistent application, and lack of diverse and engineering-informed DIs (e.g., Minor et al. 1977; Doswell and Burgess 1988; Edwards 2003). Taken together, Doswell et al. (2009) and Edwards et al. (2013) comprehensively covered the history and application of both scales, with implications for tornado climatology.

Tornado-rating practices can affect operations as well as climatological research (Weiss and Vescio 1998). Meteorological factors known to lead to higher-rated, more-destructive and generally deadlier tornadoes influence operational forecast decisions and messaging at all scales—from severe-weather outlooks to mesoscale discussions, watches, and warnings. That includes explicit probabilistic predictions of potential for certain EF-rating categories to be realized (e.g., Edwards et al. 2015; Smith et al. 2015, 2020a,b). Tornado ratings also impact risk analysis (e.g., Grazulis 1993; Concannon et al. 2000; Coleman and Dixon 2014). As such, systemic artifacts in the rating process may subvert data integrity and impact both scientific and socioeconomic users of the data in a myriad of ways, some unknown.

The F and EF scales should be analytically interchangeable. The common DI between the F and EF scales (''well built'' homes) nominally was calibrated in EF development so that any F-scale DI rated F3, for example, still would qualify as EF3 in the newer, more-precise scale. The intent (Doswell et al. 2009; Edwards et al. 2013) was to ensure a smooth transition from F to EF, thereby making tornado data from the F era essentially interchangeable with EF data, and vice versa, for research purposes, including tornado climatology. Such F–EF cross calibration ideally would prevent undesirable, secular climatological shocks (Thorne and Vose 2010), such as significant discontinuities in bulk tornadic ratings and path measures from F to EF eras. In retrospect, how well was that ideal achieved? Or put another way, what has been the EF scale's effect on tornado climatology? Our research addresses these questions.

Tornadic path-size characteristics have been used for over five decades to establish climatologies and evaluate risk (e.g., Thom 1963), and should remain important for that purpose as the built-environment footprint keeps growing in tornado-prone regions (Ashley et al. 2014; Strader et al. 2017). Path characteristics also relate to the meteorological environments in which tornadoes occur, with some longitudinal changes across the conterminous United States (Garner et al. 2021, within the EF era). As such, any systemic path-size changes in the existing tornado records will affect evaluations of both the climatology and future threats of tornadoes. To the extent those path-area trends are nonmeteorological in nature, they also can subvert the fidelity of research analyses and conclusions that do not account for them. Do such secular changes exist?

TABLE 1. Sample sizes of filtered tornado data, by F and EF (in italics) rating, in columnar bins representing 3-yr, 12-yr, and full totals. Percentages of all tornadoes within a period/column appear in parentheses. ''Any 3 average'' sums the entire 24 yr and then divides by 8 to yield an ''average'' 3-yr period.

Rating (F/EF)	1995–97	1998–2000	2001–03	2004–06	*2007–09*	*2010–12*	*2013–15*	*2016–18*	1995–2006 F	*2007–18 EF*	1995–2018 all	Any 3 avg
0	2312 (64.5)	2119 (61.1)	2266 (64.4)	2661 (63.9)	*2377 (59.1)*	*2159 (53.6)*	*1688 (55.3)*	*1794 (51.4)*	9358 (61.1)	*8018 (54.9)*	17 376 (59.2)	2172
1	889 (24.8)	923 (26.6)	878 (25.0)	1119 (26.9)	*1175 (29.2)*	*1231 (30.5)*	*1054 (34.5)*	*1331 (38.1)*	3809 (24.9)	*4791 (32.8)*	8600 (29.3)	1075
2	283 (7.9)	295 (8.5)	270 (7.7)	289 (6.9)	*349 (8.7)*	*441 (10.9)*	*230 (7.5)*	*307 (8.8)*	1137 (7.4)	*1327 (9.1)*	2464 (8.4)	308
3	77 (2.1)	103 (3.0)	82 (2.3)	85 (2.0)	*104 (2.6)*	*144 (3.6)*	*61 (2.0)*	*56 (1.6)*	347 (2.3)	*365 (2.5)*	712 (2.4)	89
4	23 (0.6)	23 (0.7)	23 (0.7)	9 (0.2)	*18 (0.4)*	*46 (1.1)*	*20 (0.65)*	*5 (0.14)*	78 (0.5)	*89 (0.6)*	167 (0.6)	21
5	2 (0.06)	3 (0.09)	0	0	*2 (0.05)*	*9 (0.22)*	*1 (0.03)*	*0*	5 (0.03)	*12 (0.08)*	17 (0.06)	2
All tornadoes	3586	3466	3519	4163	*4025*	*4030*	*3054*	*3493*	14 734	*14 602*	29 336	3667

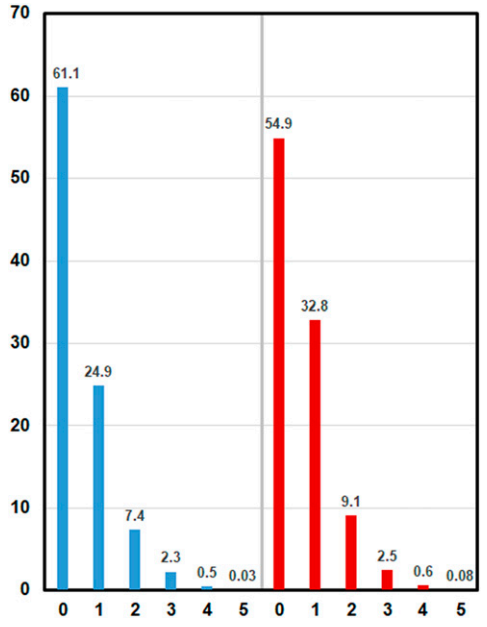

FIG. 1. Percentage of tornadoes (ordinate) of each rating (abscissa) of the F (blue) and EF (red) scales through the 1995–2018 study period, from Table 1.

Upward temporal trends in path dimensions into this century have been noticed and discussed in other research (e.g., Agee and Childs 2014; Elsner et al. 2014), and as the latter stated, ''more work needs to be done to understand the reason behind the increase in path length and width.'' Our work represents updated documentation of those trends (in the WSR-88D era), extending deeper into this century to reveal an apparent strong secular contribution to path-area increases corresponding to the change from F to EF scales. Section 2 describes data used, filters applied thereto, analysis methods, and sampling, while section 3 offers results and interpretations of our analyses. We conclude with section 4, summarizing this examination, along with its implications and recommendations for future research using U.S. tornado data.

2. Data, filtering and sorting

The WSR-88D radar network (Crum and Alberty 1993) largely was completed by 1995. The ensuing time frame represents the ''modernized'' NWS period, a time of relative stasis in data-recording procedures for tornadoes, motivated by largely WSR-88D-based warnings and verification thereof (Edwards 2012). Relative to 1950–94, this also represents an era of greater traditional-media coverage of tornadoes, the popularization and proliferation of storm chasing, consumer digital cameras, expansion of cellular communications, and (in the EF era) social media, to aid in tornado documentation. Verbout et al. (2006) discussed changes in tornado-data characteristics related to the WSR-88D, as well as prior data shifts, and emphasized using statistical detrending techniques when analyzing the entire ONETOR

TABLE 2. As in Table 1, but with counts and percentages by these damage-rating categories: Weak (F/EF0–1), strong (F/EF2–3), violent (F/EF4–5), significant (F/EF2+), and F/EF1 and 2 combined.

Rating (F/EF)	1995–97	1998–2000	2001–03	2004–06	*2007–09*	*2010–12*	*2013–15*	*2016–18*	1995–2006 *F*	*2007–18 EF*	1995–2018 all	Any 3 avg
Weak	3201 (89.3)	3042 (87.8)	3144 (89.3)	3780 (90.8)	*3552 (88.2)*	*3390 (84.1)*	*2742 (89.8)*	*3125 (89.5)*	13 167 (89.4)	*12 809 (87.7)*	25 976 (88.5)	3247
Strong	360 (10.0)	398 (11.5)	352 (10.0)	374 (9.0)	*453 (11.3)*	*585 (14.5)*	*291 (9.5)*	*363 (10.4)*	1484 (10.1)	*1692 (11.6)*	3176 (10.8)	397
Violent	25 (0.7)	26 (0.8)	23 (0.7)	9 (0.2)	*20 (0.5)*	*55 (1.4)*	*21 (0.7)*	*5 (0.1)*	83 (0.6)	*101 (0.7)*	184 (0.6)	23
Significant	385 (10.7)	424 (12.2)	375 (10.7)	383 (9.2)	*473 (11.8)*	*640 (15.9)*	*312 (10.2)*	*368 (10.5)*	1567 (10.2)	*1793 (12.3)*	3360 (11.5)	420
F/EF1 and 2	1172 (32.7)	1218 (35.1)	1148 (32.6)	1408 (33.8)	*1524 (37.9)*	*1672 (41.5)*	*1284 (42.0)*	*1638 (46.9)*	4946 (32.3)	*6118 (41.9)*	11 064 (37.7)	1383
All tornadoes	3586	3466	3519	4163	*4025*	*4030*	*3054*	*3493*	14 734	*14 602*	29 336	3667

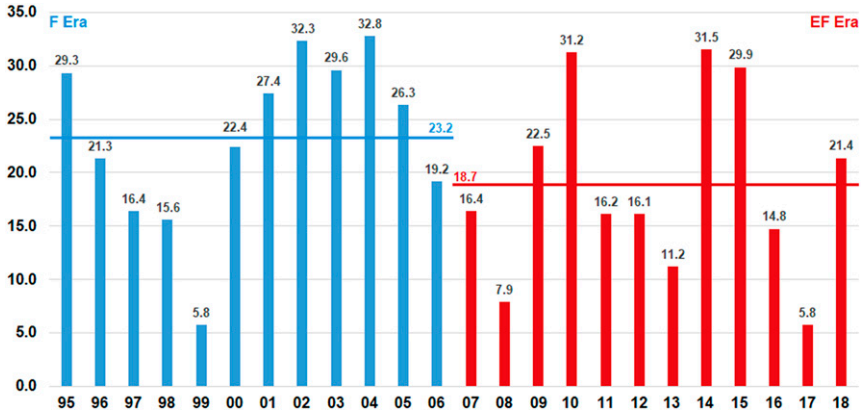

FIG. 2. Percentage (ordinate) of each year's total yeardays on which the 50th ≥F1 (blue) and then ≥EF1 (red) tornado occurred. Horizontal colored lines represent averages for the respective 12-yr F and EF periods. The leading two digits of the year are truncated on the abscissa labels.

dataset from 1950. Analyses by Agee and Childs (2014) adjusted pre-1995 path-width data upward, to account for a procedural change that year from recording mean to maximum path width. Florida-focused analyses in Elsner et al. (2018) detrended width data after the 1995 width-standard reset.

We examine relatively stable "modernized era" data-gathering practices and standards (including width), to minimize or avoid detrending, and for balance of both time sampling and tornado counts. This study follows through on the informal work of Edwards and Brooks (2010, hereinafter EB10), which compared the first 3 yr of the EF era with the last 12 yr of F. Preliminarily findings included loss of EF0 events to EF1 and EF2 bins, but path-size characteristics were not examined. Here, we restrict analyses to fundamental ONETOR variables in the WSR-88D era, and one index derived arithmetically from them, in two 12-yr bins: end of the F era from 1995 to 2006, and the 2007–18 part of the EF era. The data further are compared across eight 3-yr bins (four using F, four of EF) that are arbitrary in time-size choice but temporally balanced, and of large sample size, after EB10. Data also were examined across individual years. Because January 2007 had only 21 tornadoes (of 985 filtered events or 2.1% of the yearly tally), they are included with tornadoes for the rest of 2007 and the EF era.

Filtering was performed to expunge obviously bad or extraneous ONETOR entries, in these quantities: 33 located outside the conterminous 48 U.S. states, 562 with an unphysical value of zero for pathlength and/or width (oddly, 65% of which were in one year, 1999), and 32 with zero as latitude and/or longitude. Data with each of those problems were not used for analyses, but instead separated out for documentation, reproducibility, and potentially to inform future work outside the scope of this study. Also disused were 111 EF-unknown (EFU) entries, all from 2016 to 2018 when that category became valid in NWS *Storm Data* compilation directives. That category is meant to substitute for the legacy default practice of rating nondamaging tornadoes, or those with inaccessible paths or otherwise unknown damage, as F/EF0 (Edwards et al. 2013). The EFU rating did not come into practical use until 2016, and seldom has been applied since. Since their purpose largely is to substitute for a defined subset of EF0 ratings, one may presume that EFUs otherwise would be EF0s, and analyze them accordingly. However, given that some uncertain number of them truly may be rated due to *unknown* (as opposed to *lack of*) damage, rating-based indices should not use a nonnumeric category such as EFU, whose sample size also is small (two orders of magnitude less) relative to the dataset as a whole. As such, we simply set those aside.

The final, filtered analysis dataset contains 29 336 tornado records: 14 734 tornado records (50.2%) from 1996 to 2006 and 14 602 (49.8%) from 2007 to 2018. Table 1 provides sample-size characteristics for the resulting filtered dataset by F and EF ratings, as well as eight 3-yr subsamples analyzed in section 3. Although unsurprising natural variability in total tornado counts exists on smaller time scales, such as 1–3 yr, the remarkable and unplanned balance between the two 12-yr periods represents essentially steady bulk tornado-sampling levels between the last 12 yr of F and the first 12 yr of EF. This is consistent with the aforementioned notion of no need for detrending subsampled (1- or 3-yr) tornado counts for our purposes, *within* the conterminous WSR-88D and maximum-path-width eras. Large sample size is important in evaluating tornado data that are affected by assorted secular influences (Doswell 2007). Both the 12-yr sets ($\sim 10^4$ events) and 3-yr subsamples ($\sim 10^3$) offer that advantage.

Every tornado in the filtered 24-yr dataset has a damage-rating integer based on the F (first 12 yr) and EF (second 12 yr) scales. Doswell and Burgess (1988) discussed subjectivity and inconsistencies in F-scale ratings, demonstrated in a multiaudience teaching exercise by Edwards (2003). Despite its far-greater precision, subjectivity issues affect the EF scale also, given uncertain engineering of many specific local DIs, and the rating process's inherent dependence on judgment calls (Doswell et al. 2009; Edwards et al. 2013). Nonetheless, the 10^4 order of magnitude of tornado records

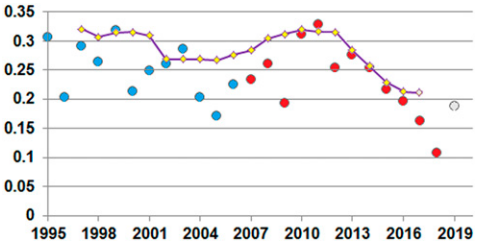

FIG. 3. Mean number of tornadoes of at least F(n + 1) damage divided by at least F(n) damage, averaged over n = 1–3, by year (dots) for the 12 F (blue) and 12 EF (red) years, as labeled on the abscissa. The ratio value is on the ordinate. Five-year running [≥F(n + 1)/≥F(n)] values are represented by yellow dots along the purple line. Preliminary 2019 values use gray fill.

in our analysis should mitigate the bulk analytic impacts of either local rating outliers or singular, nonsystemic data-entry errors in individual events.

We analyzed the filtered data via comparative absolute numbers, percentages of totals, means, medians, distributions via percentile analyses, and Weibull distribution functions. The latter functions were accumulated and plotted from the shape and scale parameter of the width and length values for each category (F and EF) and damage level 0–5. F/EF3–5 data were combined because of relatively small sampling per damage level. Weibull distributions are a useful tool in determining probability distributions and have been used to model wind speed (Wilks 1995). The Weibull distributions are given by

$$f(x) = \left(\frac{\alpha}{\beta}\right)\left(\frac{x}{\beta}\right)^{\alpha-1} \exp\left[-\left(\frac{x}{\beta}\right)^{\alpha}\right], \quad (1)$$

where α and β represent the scale and shape parameters. The shape and scale parameters were calculated in RStudio (https://rstudio.com/products/rstudio/)—an open-source package that runs the R Project for Statistical Computing (https://www.r-project.org/)—using the ''fitdistr'' formula. Once the scale and shape parameters were derived, these values were used with two functions; *dweibull*, which gives the density, and *pweibull*, which was used to calculate the cumulative density function (CDF). The *dweibull* formula was used with the same shape and scale parameters to produce the probability density functions (PDFs) for each rating level and F/EF era for the width and length. Finally, cumulative distribution functions (CDFs) were produced for the width and the length using *pweibull*. The same shape and scale parameters were used for each level (F/EF0, F/EF1, F/EF2, and F/EF3+).

3. Analytic results and interpretations

We assessed the filtered tornado data based on the following variables native to ONETOR: F or EF rating, pathlength, maximum path width, tornadic start time, deaths, and injuries. A derived, nonlinear composite parameter was used also: destruction potential index (DPI; Thompson and Vescio 1998; Doswell et al. 2006), which simply multiplies pathlength, path width, and the F or EF rating plus one (to eliminate multiples of zero). DPI has been used both as an individual

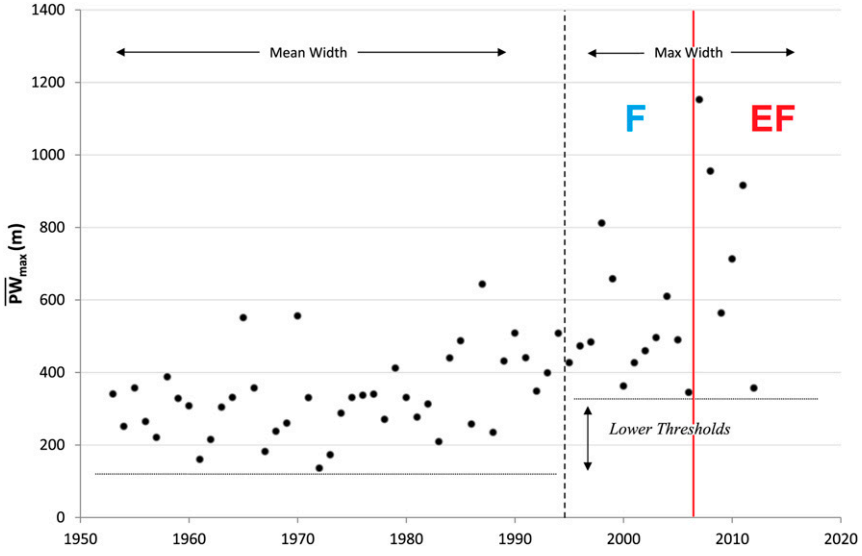

FIG. 4. An annotated version of Fig. 7 from Agee and Childs (2014), covering yearly mean significant (F/EF2+; Hales 1988) tornadic path widths (m) in their differently filtered 1953–2012 version of ONETOR. We mark the F–EF transition (red vertical line; 2007) to suggest the early stages of the EF ''shock'' to the climatology documented in the text, following the change in width standard from mean to maximum (black vertical dotted line; 1995). The initial upward change in reported widths occurred around 1990, prior to the official 1995 change in definition.

event-magnitude proxy, and as a bulk input variable to indices that compare tornado outbreaks (e.g., Doswell et al. 2006; Shafer and Doswell 2010).

a. Damage ratings

Changes in tornado climatology relative to damage rating are apparent from the F to EF periods but are more gradual than with path characteristics discussed below. Figure 1 graphically represents Table 1 percentages of tornadoes rated according to each level (0–5) in the 12-yearly F and EF periods. Table 2 parses the data in the same temporal bins as Table 1, but by grouped *classes* of damage ratings. Relative to corresponding levels in the F era, EF1 and EF2 tornadoes increased at the apparent expense of 0s, a trend that already was evident in EB10s examination of the first 3 yr of the unfiltered EF dataset. The question for EB10's very early analysis was whether that loss of F0 counts to EF1 and/or 2 was an aberration, or a continuing feature of EF rating; clearly it is the latter. However, as the gain of EF1 sampling with respect to EF0 has continued in the EF era, other variables may be exerting influence, in addition to practices involving EF rating.

A conceptual average 3-yr period for any consistently available tornadic variable can be measured by taking all eight 3-yr bins for that variable and averaging them. Three-year periods within the F and EF eras can be compared with that ''any 3 average'' (Tables 1 and 2) for evidence of systemic shifts of that variable. Among the most marked changes from the F to EF eras relative to ''any 3 average'' are three of the four EF periods being low for EF0 ratings and high for EF1s and EF2s (and of course for the combination of EF1 and 2). Trends at higher individual rating levels (as well as with violent tornadoes) are less apparent, and may be less meaningful anyway, due to relatively small sample sizes. Only half the 3-yr EF periods exceed or fall below ''any 3 average'' for conventionally grouped damage-rating classes such as weak, strong, and significant, indicating the importance of examining each large-sample rating level (i.e., EF0, EF1, and EF2) individually to better notice F-to-EF-era changes in damage-estimated tornado intensity.

One metric used by Brooks et al. (2014) to illustrate increasing U.S. tornado-occurrence variability over time is the Julian day of the 50th F/EF1 tornado within a year. This variable specifically excludes the weakest (F/EF0) events that both dominate the overall sampling and are most subject to changes in reporting practices (Verbout et al. 2006). To determine analogously if any EF-associated changes in tornadoes rated ≥1 are evident, we use a version of that measure that also accounts for years with leap days: the percentage of Julian days in the year when the 50th F/EF1 tornado was reached (Fig. 2). Although the ''50th F/EF1 tornado'' milestone has varied considerably from year to year, more variability is apparent in the EF era. The 50th EF1 tornado also has been reached 4.5% of the year (≈16 days, or just over one-half month) sooner, on average, than was the corresponding F1 tornado. We caution that the *p* value from the Mann-Whitney test (testing the probability

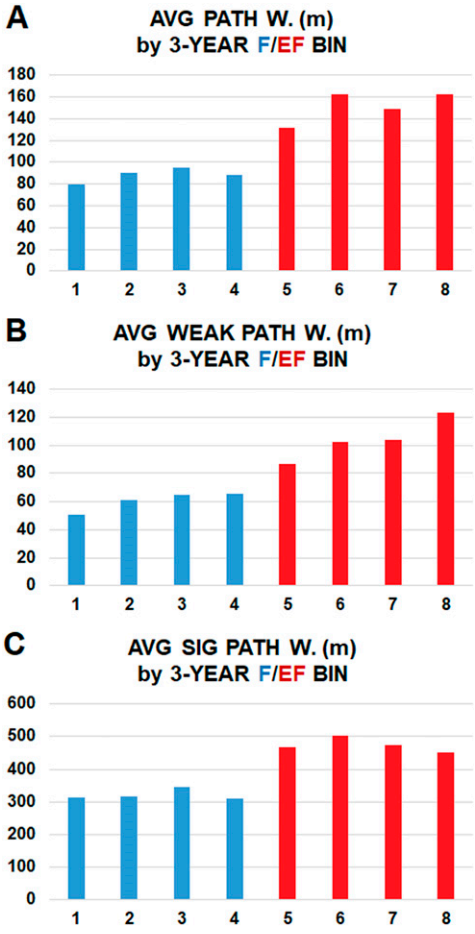

FIG. 5. Mean 3-yearly path width (m; ordinate) for (a) all, (b) weak, and (c) significant tornadoes (at least F/EF2), color-coded by chronological 3-yr F (blue) and EF (red) periods that are numbered on abscissa: 1 is 1995–97, and so on through 8, which is 2016–18.

that a value from the old era is later in the year than in the new era) is ~0.125, not traditionally statistically significant. This relates to the aforementioned interannual variability, and the greater annual tornado volume deeper into the springtime (i.e., it is harder to be late than early with year-to-year sampling at a given milestone). The extent to which the earlier average 50th EF1 by itself is purely secular (due to changes in rating practices) or climatological is unknown. Signals for earlier tornado-frequency peaks have become apparent in the central United States (Long and Stoy 2014; Lu et al. 2015), but not necessarily in the Southeast (Long et al. 2018). Our bulk mainland U.S. dataset includes both areas. Interannual tornado-frequency variability as a whole appears related to larger-scale climate aspects (e.g., Allen et al. 2018). Taken in the context of other EF-era shifts described above and below, one or more secular influence(s) is suspected, not necessarily being limited to EF itself, and alongside any from ambient climate.

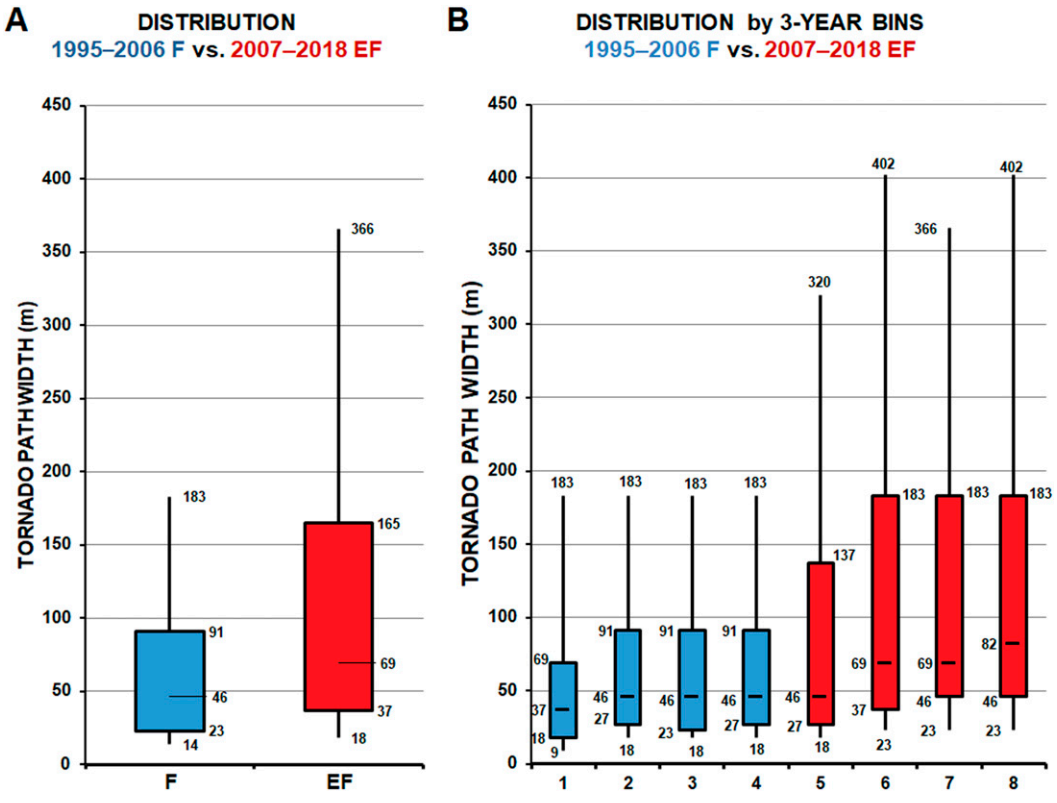

FIG. 6. Boxplots of path widths in the F (blue) and EF (red) eras, by chronological (a) 12- and (b) 3-yr bins. Boxes extend from labeled 25th to 75th percentiles around labeled median bars. Labeled whiskers extend to 10th and 90th percentiles. Frequent percentile appearance of seemingly overprecise values such as 91 or 183 m results from conversion from customarily reported imperial-unit equivalents (e.g., 100 or 200 yd, respectively). Sample sizes for these bins are given in Table 1.

In the context of multidecadal trends, a lessening of damage ratings in the early 2000s, showed by Doswell et al. (2009), is evident in our analyses. The relative consistency of tornado ratings, temporally and across multiple nations, was discussed by Brooks and Doswell (2001). Figure 1 in EB10 shows general consistency for U.S. ratings over three decades beginning in the 1980s, via counts of tornadoes at or above F/EF1. F/EF0 events were not assessed there due to the dominance of statistical results by the relatively vast population of that category (which continues in our data, per Table 1). Conversely, the minuscule number and erratic temporal occurrence of F/EF5 events precludes meaningful statistical focus on that damage level. We instead fit a linear regression from F/EF1+ through F/EF4+, whose slope can be expressed as the tornado count at one class divided by the number at the previous class. The resulting ratio $[\geq F(n+1)/\geq F(n)]$, where F can be either F or EF rating and n is 1–3, represents an answer to the following question: "Given a tornado is at least rated F(n), what's the probability it will be at least F($n+1$)?"

From 1975 to 1995 (EB10), and through the remainder of the F era, the yearly mean was about 0.25, with a general decrease throughout our 12-yr F period also evident in a 5-yr running value (Fig. 3). The decline implies a reduction of F4+ by approximately 40% in the 2000s that seems unlikely to be meteorologically driven, given the relative consistency in pre-WSR-88D years (EB10). Yet the running value increased for a few years upon EF onset, before starting an unprecedentedly steep decline in 2013 that has continued since. The 2017 and 2018 yearly means are the lowest on record since the NWS has rated tornadoes using the F and EF scales, with the ratio nearly as low as 0.10 in 2018 (the last year of our sample), a precipitous drop to less than 1/3 of

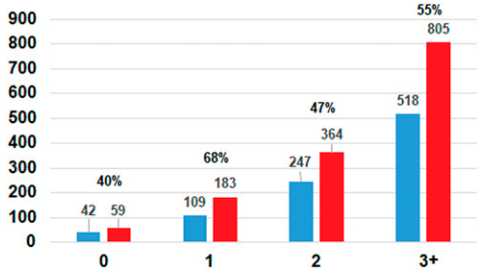

FIG. 7. Average path widths (m; ordinate) in the F (blue) and EF (red) eras by damage rating (abscissa). Overhead percentages represent EF increases over F values. Sample sizes by rating are in Table 1.

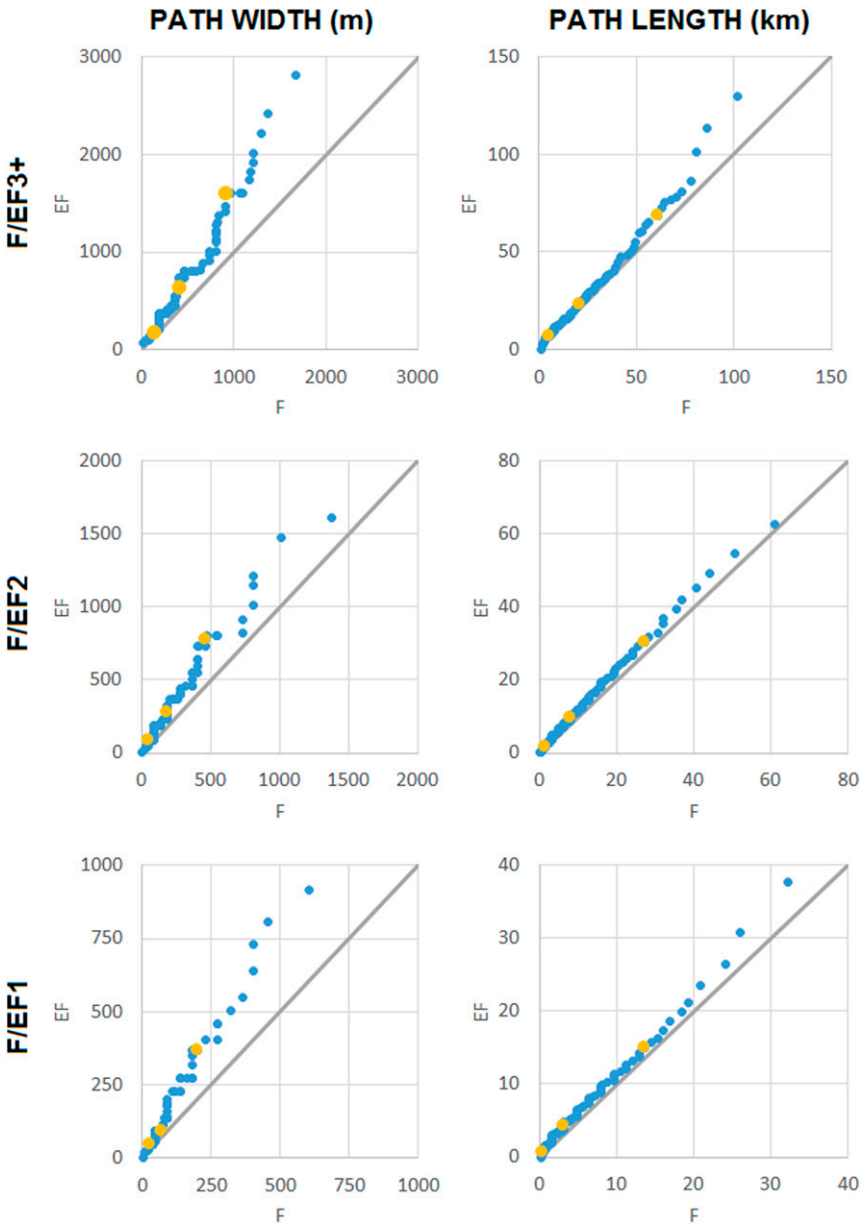

FIG. 8. Scatterplots of width and length distributional percentiles (top labels), for rating categories (left labels) in the F (abscissas) and EF (ordinates) eras. Each dot is a percentile from 0 to 99, with the goldenrod color representing 10th, 50th, and 90th percentiles.

the peak value in the historically upper-echelon (Doswell et al. 2012) tornado year of 2011.[1]

Factors contributing to this relative decline are unclear, and a matter of speculation, given the lack of metadata noted above. Still, the trend indicates strong bulk secular influence on damage ratings that is temporally coincident with nationwide retrofitting of dual-polarization capabilities to the WSR-88D network—specifically, the ability to detect tornadic debris signatures (TDSs; Ryzhkov et al. 2005), whose plume characteristics have been related statistically to damage rating (Bodine et al. 2013). The extent to which TDSs may *influence* subsequent rating is undocumented, and no causal linkage is either quantifiable or posited here. Still, at a minimum, TDS appearance invokes near-certainty of a tornado in real-time operations, reveals target areas for damage surveys, and offers presurvey

[1] Preliminary examination of 2019 data (added to Fig. 3) shows a minor reversal of the ratio to a value ≈ 0.19, which is still lower than all but one on the F era and is below average even for the EF era.

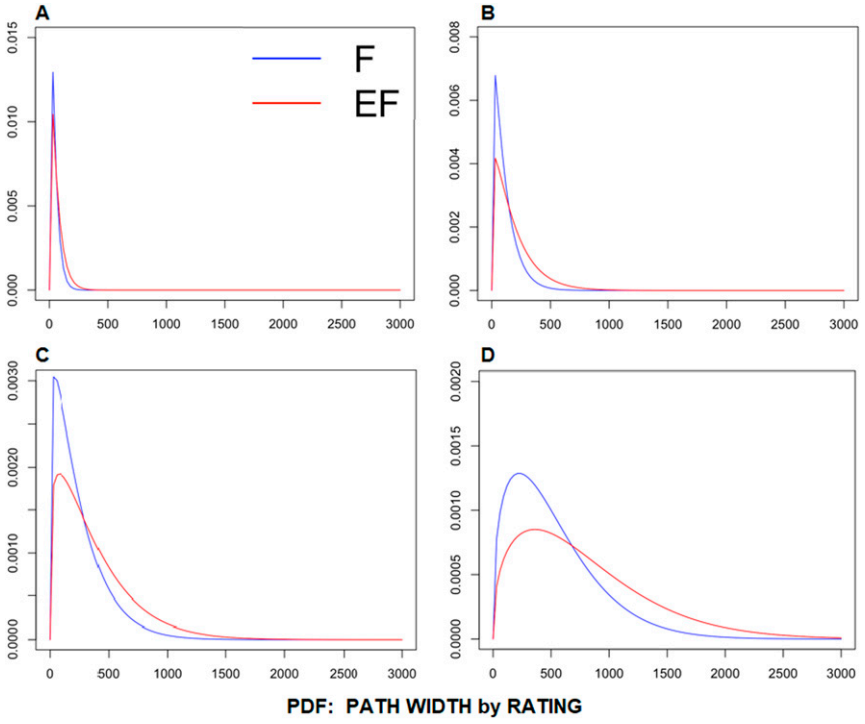

FIG. 9. Probability density function (ordinates) for width (m; abscissas) by F/EF rating for the (a) F/EF0, (b) F/EF1, (c) F/EF2, and (d) F/EF3+ bins used in Fig. 8. The blue line represents probability of occurrence in the F era, and the red line represents the same for the EF era.

information on *potential* damage intensity, as does operational recognition of other radar signatures in concert with environmental parameters (Smith et al. 2015).

b. Path characteristics

1) WIDTH

Following an increase in the WSR-88D era related to the 1995 change to max width (as discussed above), another transitional jump in path width appeared in the late 2000s significant-tornado subset of the Agee and Childs (2014) analyses (Fig. 4). That increase was noticed and described as "a recent uptick toward wider tornadoes." However, they did not associate the phenomenon explicitly with contemporaneous EF usage.

In our analyses, path widths similarly have increased in the larger sampling of the EF era for weak (EF0–1) as well as significant tornadoes. Mean F to EF path width for all tornadoes increased from 89 to 151 m, a 170% increase. Though quite strongly apparent when plotting yearly means (not shown), the 3-yr bins, which smooth away natural year-to-year variability, reveal that this change also was relatively sudden, appearing essentially stepwise in character from the F to EF eras (Fig. 5) across all tornadoes, as well as weak and significant tornadoes. Within the EF era, weak-tornado path widths (Fig. 5b) markedly increased again in the last bin (2016–18), comparable to those from F to EF; their 123-m average was 241% of that during 1995–97.

Distributions of both 12-yr and 3-yr path-width subsamples (Fig. 6) also illustrate the marked increase in reported width in the EF era, especially at median and larger values. Path widths in the EF data skewed upward by about half a quartile relative to F-scale tornadoes, for the middle quartiles. Though widths increased abruptly across the F to EF transition, they have enlarged within the EF era also. Recorded tornado widths for 2016–18 were over twice those of 1995–97 *at every percentile sampled*: 10th, 25th, 50th, 75th, and 90th, across similar counts of ≈3500 tornadoes. The 90th percentile (whisker tip) value of every 3-yr F bin—183 m (200 yd)—matched the 75th percentile of each bin in the last 9 yr of the EF data.

Average path widths by rating increased across all bins, by 40%–68% from F to EF, with the largest percentage growth in EF1s. Path-width expansion in absolute terms has been especially pronounced between the F and EF eras for strong to violent tornadoes, as suggested by Figs. 5c and 7, with reported widths for EF3+ tornadoes nearly 300 m larger than for F3+. The widest year for average path of significant tornadoes (568 m) was 2011—the aforementioned, anomalously outbreak-driven year, while the narrowest was 282 m in 1999 (despite already having filtered out an inexplicably large number of zero-width tornado-entry errors that year, including 27 that were significant). Strikingly, *in none of the F years sampled did the yearly mean of significant-tornado widths reach that for the EF year with the narrowest mean of width* (386 m in 2012; not shown).

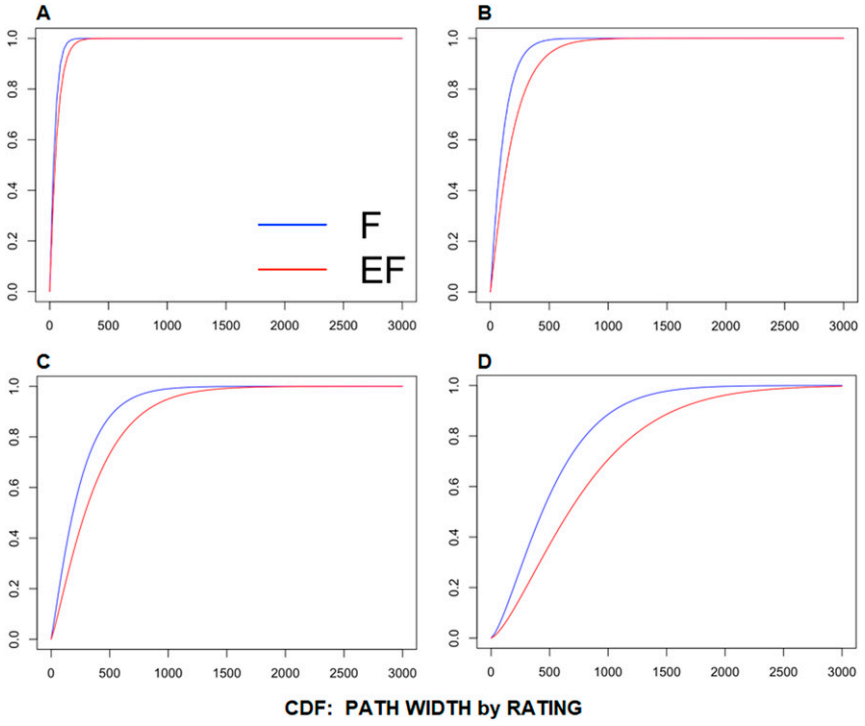

FIG. 10. As in Fig. 9, but for cumulative distribution function, representing the probability of a value being less than or equal to a given width.

A comparison of 100 F and EF path-width percentiles for F/EF3+ events (Fig. 8), taken at whole integers, shows that the EF expansion of recorded tornado width systemically strayed farther from the ideal ''no change'' line as percentiles enlarged and approached 100. Subsampling of the EF era indicates a marked jump occurred in weak-tornado widths during the final period, 2016–18 (Fig. 5b), which presently defies evidential explanation. Monitoring over several more years will be needed to determine if the 2016–18 weak-width jump is a ''shock'' within the EF era, or an anomaly confined to that 3-yr period.

Overall, for width (Fig. 9), the Weibull graphs' shape and scale parameters increase with the EF scale. This indicates that the maximum probability moves away from zero with the higher EF. The shift toward wider paths at all ratings—but especially for significant tornadoes—manifests in these probabilities of occurrence as well. The higher the F/EF, the more separated they are, which is also evident in the cumulative distribution functions (Fig. 10).

2) LENGTH

Paths have elongated overall from the F to EF eras (e.g., Fig. 11), though length changes are smaller than width changes. Average pathlengths by 3-yr bin increased for all tornadoes and weak tornadoes, but not necessarily for strong to violent events (Fig. 11c). In fact, when removing the influence of the anomalously intense 2011 season (Doswell et al. 2012) on the bin-6 (2010–12) data, the disproportionate influence of weak tornadoes on pathlength expansion becomes even more pronounced (not shown). For weak tornadoes, no 3-yr bin in the F era contained lower average pathlength than *any* bin in the F era. The same can be stated about tornadoes overall, but that is clearly related to the sample-size dominance of weak tornadoes (Fig. 11 and Table 2 taken together).

Distributions of F and EF pathlengths (Fig. 12) show more interquartile overlap than for width, but still, across-the-board increases from the F to EF eras at all percentiles sampled at and above the median. Coarsely averaging lengths by EF rating from the F to EF eras, increases are quite apparent (Fig. 13), but not as great as widths in terms of percentage jumps (cf. Fig. 7). The 2011 season largely contributes to the EF3+ increase in widths by this measure as well, through its anomalously high occurrence of long-tracked, strong-to-violent tornadoes across multiple outbreaks (Doswell et al. 2012); however, the upward shifts in length at lower rating levels are more consistent throughout the rest of the EF era. As with width, the bulk increases in the distributions and averages of length directly coincided with the beginning of the EF era, appearing as a stepwise jump. However, lengthening of paths by multiple kilometers is more difficult to explain, as compared with observed widening by tens to hundreds of meters, in light of such factors as EF-compelled DI variegation or greater storm-surveying precision. One contributor may be the expanding built footprint of DI targets (e.g., Ashley et al. 2014; Ashley and Strader 2016), though more across decades than instead of across a relatively short-fused procedural discontinuity such as imparted by the EF adoption.

As with width, Weibulls' shape and scale parameters for length increased with more-intense F/EF bins, similarly indicating probability movement away from zero with greater rating (Fig. 14). As expected from the above results for length, there is not much variability within the Weibulls for different rating levels. Unsurprisingly, the Weibulls show the highest probability of lengths <10 km for weak to marginally significant bins (F/EF0–F/EF2). As the ratings increase, the probability increases with a majority of EF3+ tornadoes reaching longer lengths. These plots also decrease exponentially with more uncertainty and variability for the F/EF3 tornadoes. In comparing the F with EF it is seen that, unlike the width values, they are not well separated and show similar probabilities across most lengths and ratings. The CDFs (Fig. 15) also show a similar pattern, as the distributions tend toward longer length with greater rating, but less separation between F and EF, relative to tornado-damage width.

3) DPI

With DPI incorporating length, width and rating, all of whose magnitudes have shifted upward to varying extents (above), growth in those components should and does manifest strongly in this bulk index. DPI for significant tornadoes can be multiple orders of magnitude larger than for the smallest, weakest ones—especially individually, but even in a bulk sense (cf. ordinates in Fig. 16). As such, analyses of this measure disproportionately favor the influence of the largest, longest-lived and most intensely damaging tornadoes, despite the much-larger absolute counts of weak, relatively brief events. That is apparent in comparing the individual panels in Fig. 16, where the influence of the extreme 2011 year within bin 6 again shows, as it does in year-to-year comparisons of average DPI (not shown).

Still, DPI increased essentially across the board in the EF era, including for weak tornadoes. To depict these trends in data distributions graphically and legibly on one page, given the innate nonlinearity of DPI with respect to rating (i.e., the large range of magnitude from the weakest, shortest paths to strongest, longest paths), we employed logarithmically scaled boxplots (Fig. 17).[2] Although substantial interquartile overlap is apparent in the nonlinear boxplots, a consistent upward shift is apparent, commensurate with that of the width and length components (path areas), in particular. More-subtle changes in rating behavior (discussed above) are far less influential in this depiction. Still, mean DPI increased by ≈100% (or doubled) in *corresponding* F and EF ratings (Fig. 18).

As with DPI components, no explanation is apparent for an abrupt increase in actual ''destruction potential'' of tornadoes between F and EF eras, leaving the stepwise and apparently secular leap in DPI as a cautionary statement about data integrity (see more in section 4). This also underscores the need for caution in using bulk indices in terms of keenly understanding their components' influences for research purposes, as well as for forecasting (Doswell and Schultz 2006).

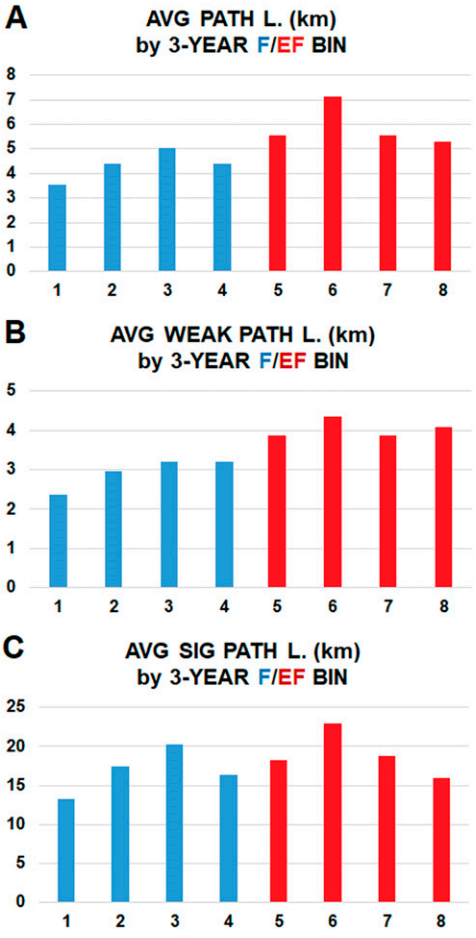

FIG. 11. As in Fig. 5, but for pathlength (km).

c. Other tornado characteristics

Other variables in ONETOR include deaths, injuries and reported tornadogenesis time. We analyzed some aspects of these with respect to the F and EF eras, with largely indefinite results. Violent tornadoes tend to cause many more casualties (deaths and injuries) than others, and deaths and injuries per tornado tend to increase logarithmically between the weakest and most violent. Figure 19 shows a mix of decreasing and increasing casualty rates per tornado from F to EF eras within ratings. However, values at F/EF4 and F/EF5 levels should be interpreted with great caution, because of their relatively small sample sizes (Table 1).

In terms of tornado times, data were binned in 3-hourly start-time ranges similar to diurnal climatology of tropical cyclone tornadoes (e.g., Fig. 5 and accompanying discussion in Edwards 2012). With the central and eastern time zones climatologically dominating tornado occurrence in the conterminous United States (not shown), minor apparent

[2] Another benefit of filtering tornadoes of unphysical zero pathlength and/or width was to avoid zero-DPI data, which of course could not be assessed in a logarithmic manner.

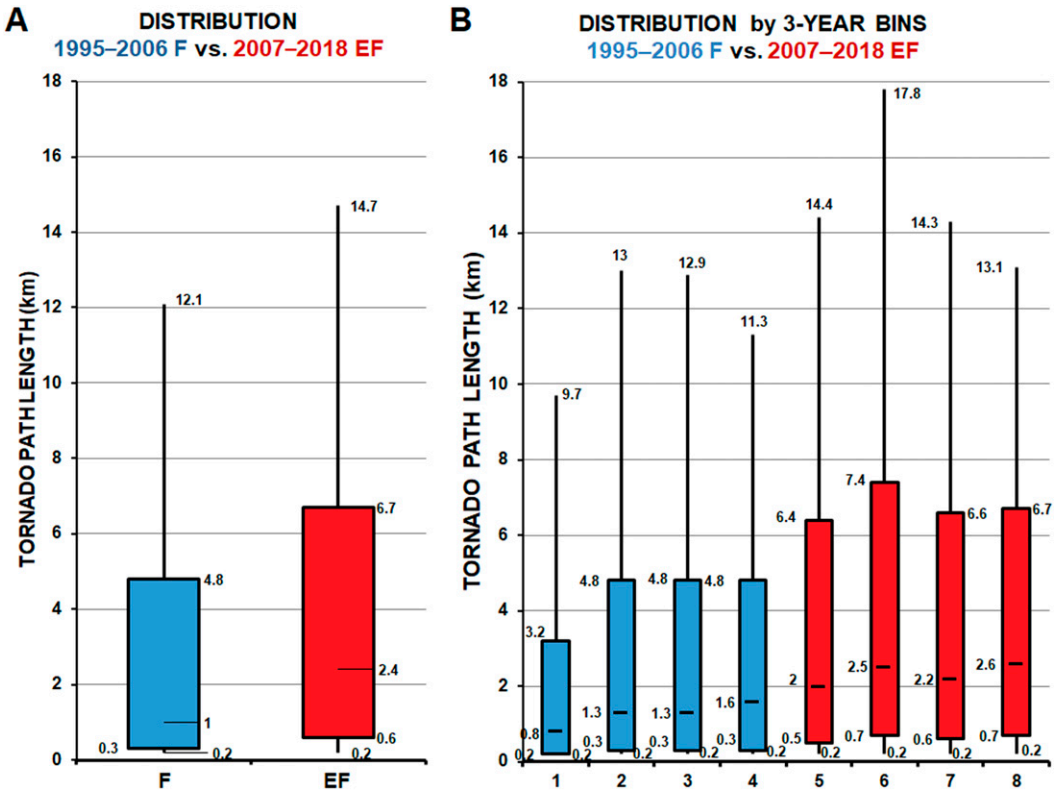

FIG. 12. As in Fig. 6 but for pathlength (km).

gain of tornadoes in the EF era during local overnight and early morning (corresponding to 0300–1459 UTC) is apparent (Fig. 20), at the expense of the climatological diurnal peak in late local afternoon to early evening periods encompassing 2300–0259 UTC. Whether this minor temporal reallocation of tornadoes to later hours is climate influenced, coincidental, or somehow related to EF practices is indeterminate.

4. Summary and discussion

With regard to evaluating tornado data, Doswell (2007) stated, ''Establishing the level of confidence in conclusions from the data cannot be done by rote. Careful consideration of data quality issues is also important in attempting to draw conclusions from data analysis.'' That statement was published less than a year after the end of the F scale, and the EF-era data have validated it further.

Procedurally, simply by virtue of greater numbers of DIs and mandated evaluation of degrees of damage within each DI, the switch to the EF scale affected damage-rating practices for tornadoes. Those changes, however, occurred amidst relatively large interannual variability in the distribution of tornado ratings. For example, the years just prior to the F–EF transition contained historically low numbers of significant tornadoes, likely as the result of changes in subjective assessment practices. As such, the EF-scale adoption, with its more procedurally structured evaluations via degrees of damage within DIs, contributed to a slight increase in assessed EF1 to EF2 damage ratings as found herein, resembling distributions from the mid-1970s to the late 1990s in ONETOR. The apparent increase in influence of nonmeteorological influences on EF1 tornado counts—a phenomenon not necessarily obvious in earlier, more-partial sampling such as Fig. 1 of Brooks et al. (2014)—casts some doubt on the validity of continuing analyses of EF1+ data for longer-term climatological assessments of tornadoes, barring some sort of EF-associated detrending of the data.

The F-era relationship of tornado path width and length to rating (Brooks 2004) is cast in greater uncertainty by the secular changes in those characteristics starting in the late 2000s. Applications, such as modeling the footprint of damage from tornadoes for risk assessment purposes, need to take into account the changes in path characteristics in

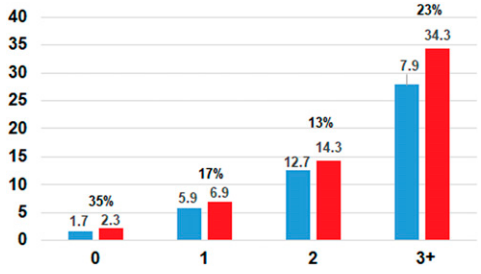

FIG. 13. As in Fig. 7 but for pathlength (km).

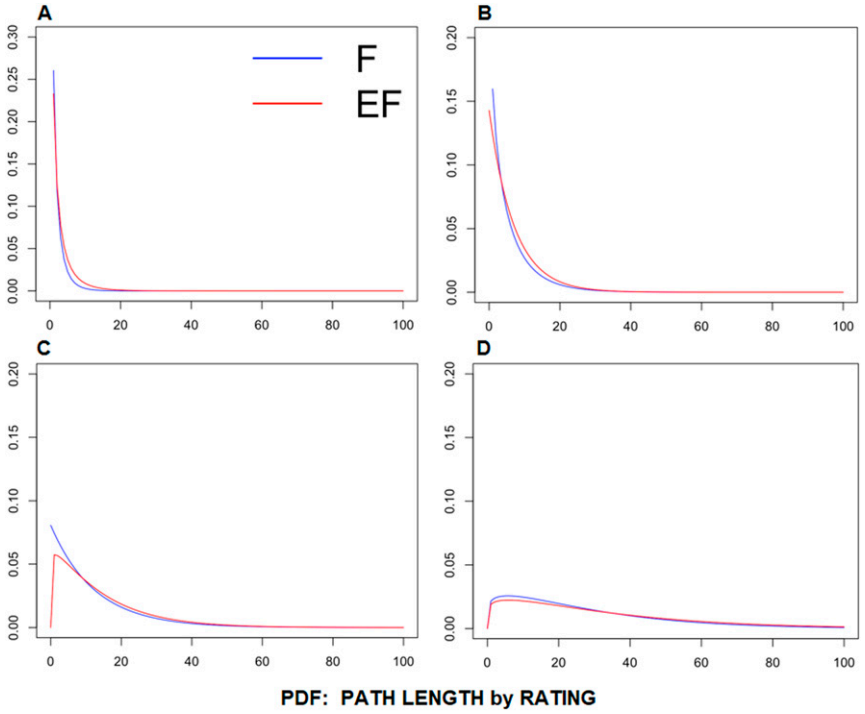

FIG. 14. As in Fig. 9, but for pathlength (km).

the EF era. It may be possible to adjust length and width between the two eras by some statistical process but, if not, sample sizes will be limited. Given the particularly large changes in width, anything that uses width without accounting for the abrupt change should be viewed with caution. Detrending for width should be done, whether by simple reduction methods comparable to Elsner et al. (2018) for post-1995 data, or via more statistically nuanced approaches.

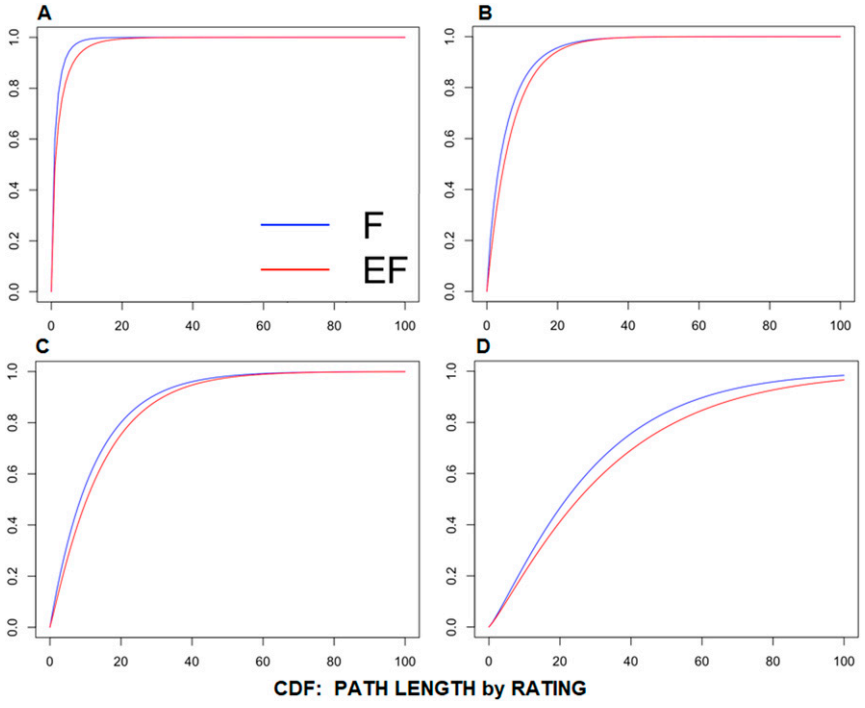

FIG. 15. As in Fig. 10, but for pathlength (km).

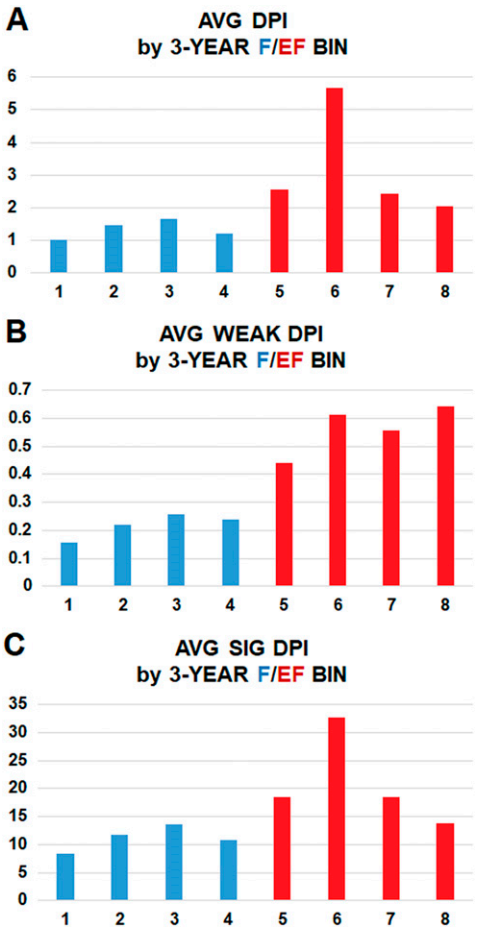

FIG. 16. As in Fig. 5, but for DPI (unitless).

An abrupt increase in path footprint (width, and to a much-lesser extent length) with the EF scale has important implications for research using path analyses. For example, path area—along with wind-field characteristics inferred from midpoint wind estimates provided by F and EF ratings—forms a basis for an index of tornadic energy dissipation or ''power'' (Fricker et al. 2017) used to infer bulk climatological changes in tornadic destruction potential over time. To that end, Fig. 1 in Elsner et al. (2019), which plots annual 50th and 90th percentiles of the same ''power'' index from 1994 to 2016, shows a gradual increase through the F era to an EF-era plateau, such that *no* year in the F era exceeds the *lowest* ''power'' year in the EF era. Further, their distributional Fig. 2a shows a striking, approximately threefold increase in median tornadic energy dissipation from F to EF eras, with no overlap in inner quartiles. However, these changes are not explicitly compared therein with the abrupt secular shifts in influential path characteristics, namely width, which clearly will affect path-area-based indexing (including DPI, as we show).

Path width has been shown to relate to environmental meteorological variables such as CAPE and 0–1-km AGL hodograph curvature within the EF era (Garner et al. 2021). No known changes exist in the atmosphere's regulation of tornado size over the 24-yr period of our examination, however, much less any shifts so abruptly across its middle. Instead, the time match of the width and length discontinuities with EF implementation, and the continuance of similarly greater path sizes thereafter, suggest that substantial, systemic influences of EF rating practices have imprinted themselves on path-dimension (along and across) climatology. Spatial shifts in favorable tornado environments east-northeastward from the southern and central plains (e.g., Gensini and Brooks 2018) have been documented on decadal climate time scales, but physical relationship of geography to path width is less clear. Width inflation may be associated speculatively to much-finer DI texturing in the EF era; however, effects not related to the ''well-built house'' DI commonly were used to mark paths before EF implementation (e.g., Edwards et al. 2013 and several citations therein).

The smaller, but still abrupt, F–EF pathlength inflation is even more difficult to explain. The *Storm Data* metadata, unfortunately, are largely short-to-nonexistent text narratives, too inconsistent in both format and stated survey reasoning (if any) to quantify specific influences within EF surveying procedures, nor do they contain any other systematic tornado-documentation effects that could be uniquely contemporaneous to the EF era, to suggest specific causes for the readily apparent EF influence on path characteristics. We also have not the evidence yet to say, for example, which era of path width (F or EF) is closer to ''correct'' for real tornadoes, especially since widths typically are imprecise estimates divisible by 50, in recorded units of yards (in the customary imperial unit, 85% of F tornadoes and 80% from the EF period had an ending digit of zero).

What only can be fodder for speculation, is this question: What about the EF scale has driven its share of these shifts in recorded tornado characteristics? The tornado data do not contain enough metadata across the entire period to quantify such influences. For example, to what extent is an increase in nominal DIs directly responsible for expanding the path footprint lengthwise, and especially laterally? While mapping and photography from the Damage Assessment Toolkit (DAT; Camp 2008; Burgess et al. 2014) began in 2009 and has become available commonly for tornadic surveys, its execution has been inconsistent, in terms of not all tornadoes being directly surveyed. Furthermore, in our 12-yr subset of the F era, finescale path metadata comparable to those resulting from use of the toolkit does not exist for all but a few notable, highly impactful events [e.g., the 3 May 1999 tornadoes, per Marshall (2002) and Speheger et al. (2002)]. What effects on survey detail and path size have arisen from the human element of finer-scale EF training and survey support internal to NWS (Edwards et al. 2013), such as from widespread usage of mobile field software and the DAT? What role has the mass proliferation of social media and smartphones, as well as advances in high-resolution

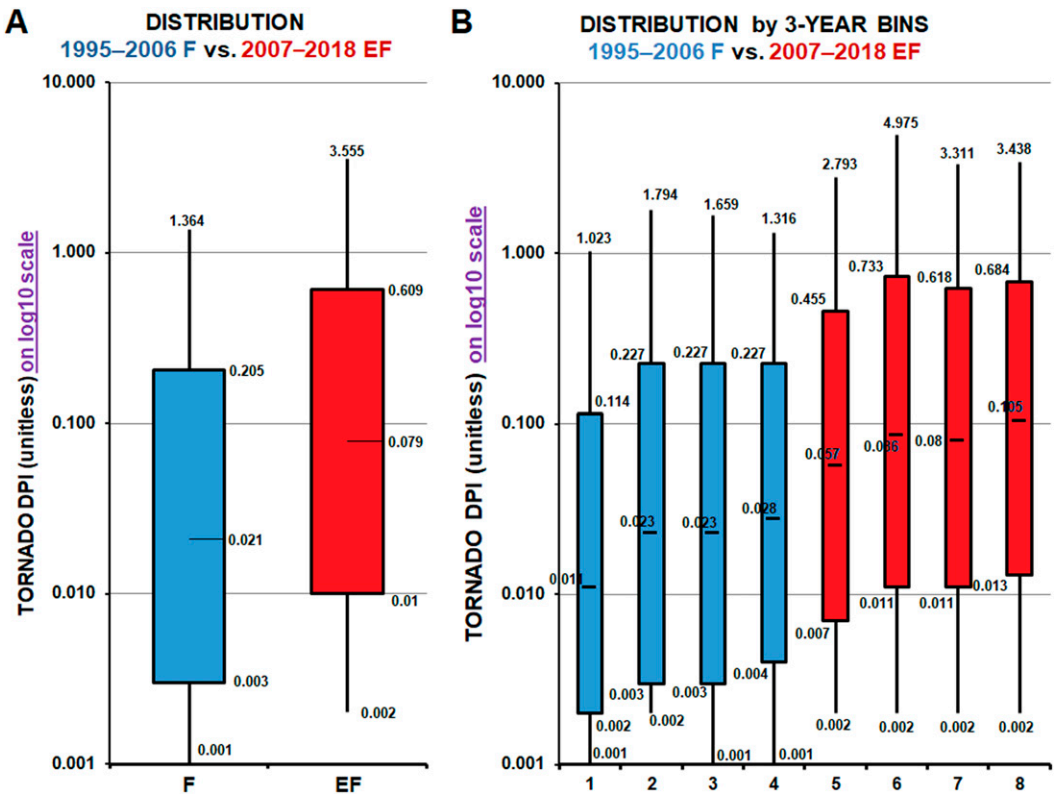

FIG. 17. As in Fig. 6 but for DPI (unitless). A *logarithmically scaled* ordinate is used because of strong DPI nonlinearity.

satellite-image interrogation (e.g., Molthan et al. 2020), and consumer-grade unmanned aerial vehicles (''drones'' or ''unpiloted aerial systems''; Wagner et al. 2019)—all broadly conterminous with the EF scale—collectively played in finding and rating EF DIs that may have been missed in the F era?

Perhaps many years of nationwide DAT usage, and related finer texturing of integrated DI details along paths, will permit future research to extract evidence for a cause of path-characteristic changes *within* the EF era, even as retrospective finescale reanalyses for a large sample of F-era tornadoes remains strongly unlikely. Regardless, for analytic purposes, bulk tornado-path data should be detrended across 2006–07 to account for either narrower, shorter tracks before EF implementation, or wider, longer ones since. Methods used in Agee and Childs (2014) and Elsner et al. (2018, 2019) may accomplish this. As Doswell (2007) noted, even under the uncertain assumption that the EF scale has ''improved'' tornado data-gathering and intensity estimation, decades more of data may need to be accumulated to ascertain less-obvious or subsampled spatiotemporal trends that are potentially pertinent to climatological analysis (as compared with the large-sample, bulk findings herein). Geospatial analysis of F characteristics versus EF characteristics was outside the scope of our study, acknowledging geographic nonuniformities in both path variables and path-size time trends. Since 1) geographic distinctions may exist in EF rating and application across NWS warning domains and/or regions, 2) path characteristics climatologically vary by state or region, and 3) decadal-scale geographic shifts in U.S. tornado-favoring environments have been documented (e.g., Gensini and Brooks 2018), such analysis may be worth undertaking—as long as the Doswell (2007) cautions are well heeded with regard to shrunken (sub)sample sizes and comparisons made therewith.

The F–EF change may not be the last nonmeteorological ''shock'' to bulk tornado records, regardless of whether the additional path-width expansion in 2016–18 endures. As of this writing, the EF scale still includes only its original DIs, with NWS ratings officially considering other factors (non-EF DIs and sensor measurements). Further enhancements

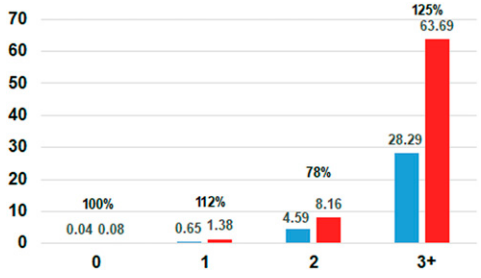

FIG. 18. As in Fig. 7 but for DPI (unitless).

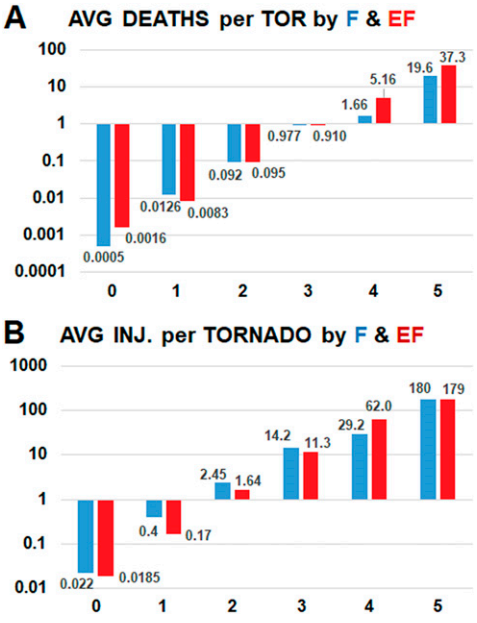

FIG. 19. Average number of (a) deaths and (b) injuries (ordinate; logarithmic) per tornado at each rating (abscissa) for the full F (blue) and EF (red) periods.

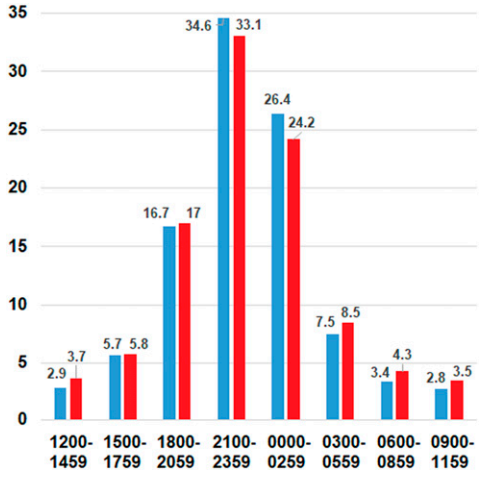

FIG. 20. Percentage (ordinate) of tornadoes in the F (blue) and EF (red) periods during 3-hourly UTC time bins prescribed on the abscissa. Diurnal and nocturnal periods in the conterminous U.S. central and eastern time zones roughly correspond to 1200–2359 UTC (left side) and 0000–1159 UTC (right side), respectively.

by a committee of meteorologists and engineers are underway for tornado rating in a years-long, collaborative undertaking under the umbrella of both the American Meteorological Society (AMS) and ASCE (LaDue 2016; LaDue et al. 2018). This includes consideration of in situ and mobile-radar wind detections, other remote sensing, treefall patterns, forensic case examinations, and new DIs in the EF scale. Assuming the committee recommendations ultimately take effect at one time, their implementation as an effectively adjusted EF scale should be monitored for further associated climatological shifts in tornadic path and rating characteristics.

Although it ideally was not supposed to occur (Edwards et al. 2013), tornado data clearly have undergone pronounced changes associated with EF damage-survey practices. For most purposes, bulk discontinuities associated with the EF scale should be acknowledged and statistically normalized in pertinent climatological analyses of tornado data. Furthermore, the relatively abrupt, essentially stepwise changes in tornadic path characteristics across the F–EF divide, and the apparent influence of updated tornado-survey practices thereon, either mask or complicate the identification of more-subtle climatic signals. This poses a substantial handicap for attempts to determine relationships (if any) between climatic change and indicators of tornado strength (i.e., damage rating), size, longevity, and numbers in the United States. A fundamental lesson for climate analyses involving tornadoes, thereby, is strongly reinforced: *understand and account for secular influences on the data.*

Acknowledgments. Insightful discussions with these scientists (in alphabetic order) benefited the study: Greg Carbin, Chuck Doswell, Tom Grazulis, Jared Guyer, John Hart, Patrick Marsh, Bryan Smith, Rich Thompson, and Steve Weiss. We thank those who have maintained and updated the public-domain tornado data at SPC and its predecessors, including (in alphabetic order) Greg Carbin, Matt Elliott, John Halmstad, David Higginbotham, Leo Grenier, Donald Kelly, Laurence Lee, Patrick Marsh, and Dan McCarthy. The SPC Science Support Branch and NSSL provided hardware and software to enable this work. Some of the material and ideas herein were adapted from a very preliminary, informal conference paper (EB10). Israel Jirak (SPC) offered valuable internal review of the paper. Suggestions by four formal reviewers (Maria Molina, James Elsner, and two who were anonymous) helped to make this work publishable and are greatly appreciated. Disclaimer: The scientific results and conclusions, as well as any views or opinions expressed herein, are those of the author(s) and do not necessarily reflect the views of NOAA or the Department of Commerce.

Data availability statement. Filtered tornado data are public domain and are available from the lead author. Unfiltered tornado data are freely available at SPC (https://www.spc.noaa.gov/wcm/#data).

REFERENCES

Agee, E., and S. Childs, 2014: Adjustments in tornado counts, F-scale intensity, and path width for assessing significant tornado destruction. *J. Appl. Meteor. Climatol.*, **53**, 1494–1505, https://doi.org/10.1175/JAMC-D-13-0235.1.

Allen, J. T., M. J. Molina, and V. A. Gensini, 2018: Modulation of annual cycle of tornadoes by El Niño–Southern Oscillation. *Geophys. Res. Lett.*, **45**, 5708–5717, https://doi.org/10.1029/2018GL077482.

Ashley, W. S., and S. M. Strader, 2016: Recipe for disaster: How the dynamic ingredients of risk and exposure are changing the

tornado disaster landscape. *Bull. Amer. Meteor. Soc.*, **97**, 767–786, https://doi.org/10.1175/BAMS-D-15-00150.1.

——, ——, T. Rosencrants, and A. J. Krmenec, 2014: Spatiotemporal changes in tornado hazard exposure: The case of the expanding bull's-eye effect in Chicago, Illinois. *Wea. Climate Soc.*, **6**, 175–193, https://doi.org/10.1175/WCAS-D-13-00047.1.

Bodine, D. J., M. R. Kumjian, R. D. Palmer, P. L. Heinselman, and A. V. Ryzhkov, 2013: Tornado damage estimation using polarimetric radar. *Wea. Forecasting*, **28**, 139–158, https://doi.org/10.1175/WAF-D-11-00158.1.

Brooks, H. E., 2004: On the relationship of tornado path length and width to intensity. *Wea. Forecasting*, **19**, 310–319, https://doi.org/10.1175/1520-0434(2004)019<0310:OTROTP>2.0.CO;2.

——, and C. A. Doswell III, 2001: Some aspects of the international climatology of tornadoes by damage classification. *Atmos. Res.*, **56**, 191–201, https://doi.org/10.1016/S0169-8095(00)00098-3.

——, G. W. Carbin, and P. T. Marsh, 2014: Increased variability of tornado occurrence in the United States. *Science*, **346**, 349–352, https://doi.org/10.1126/science.1257460.

Burgess, D. W., and Coauthors, 2014: 20 May 2013 Moore, Oklahoma, Tornado: Damage survey and analysis. *Wea. Forecasting*, **29**, 1229–1237, https://doi.org/10.1175/WAF-D-14-00039.1.

Camp, P. J., 2008: Integrating a geographical information system into storm assessment: The southeast Alabama tornado outbreak of 1 March 2007. *24th Conf. on Interactive Information Processing Technologies*, New Orleans, LA, Amer. Meteor. Soc., P1.4, https://ams.confex.com/ams/pdfpapers/134401.pdf.

Coleman, T. A., and P. G. Dixon, 2014: An objective analysis of tornado risk in the United States. *Wea. Forecasting*, **29**, 366–376, https://doi.org/10.1175/WAF-D-13-00057.1.

Concannon, P. R., H. E. Brooks, and C. A. Doswell III, 2000: Climatological risk of strong to violent tornadoes in the United States. *Second Symp. on Environmental Applications*, Long Beach, CA, Amer. Meteor. Soc., 212–219.

Crum, T. D., and R. L. Alberty, 1993: The WSR-88D and the WSR-88D operational support facility. *Bull. Amer. Meteor. Soc.*, **74**, 1669–1687, https://doi.org/10.1175/1520-0477(1993)074<1669:TWATWO>2.0.CO;2.

Doswell, C. A., III, 2007: Small sample size and data quality issues illustrated using tornado occurrence data. *Electron. J. Severe Storms Meteor.*, **2** (5), https://ejssm.org/archives/wp-content/uploads/2021/09/vol2-5.pdf.

——, and D. W. Burgess, 1988: On some issues of United States tornado climatology. *Mon. Wea. Rev.*, **116**, 495–501, https://doi.org/10.1175/1520-0493(1988)116<0495:OSIOUS>2.0.CO;2.

——, and D. M. Schultz, 2006: On the use of indices and parameters in forecasting severe storms. *Electron. J. Severe Storms Meteor.*, **1** (3), https://ejssm.org/archives/wp-content/uploads/2021/09/vol1-3.pdf.

——, R. Edwards, R. L. Thompson, J. A. Hart, and K. C. Crosbie, 2006: A simple and flexible method for ranking severe weather events. *Wea. Forecasting*, **21**, 939–951, https://doi.org/10.1175/WAF959.1.

——, H. E. Brooks, and N. Dotzek, 2009: On the implementation of the enhanced Fujita scale in the USA. *Atmos. Res.*, **93**, 554–563, https://doi.org/10.1016/j.atmosres.2008.11.003.

——, G. W. Carbin, and H. E. Brooks, 2012: The tornadoes of spring 2011 in the USA: An historical perspective. *Weather*, **67**, 88–94, https://doi.org/10.1002/wea.1902.

Edwards, R., 2003: Rating tornado damage: An exercise in subjectivity. *First Symp. on F-Scale and Severe-Weather Damage Assessment*, Long Beach, CA, Amer. Meteor. Soc., P1.2, https://ams.confex.com/ams/pdfpapers/55307.pdf.

——, 2012: Tropical cyclone tornadoes: A review of knowledge in research and prediction. *Electron. J. Severe Storms Meteor.*, **7** (6), https://ejssm.org/archives/wp-content/uploads/2021/09/vol7-6.pdf.

——, and H. E. Brooks, 2010: Possible impacts of the enhanced Fujita scale on United States tornado data. *25th Conf. on Severe Local Storms*, Denver, CO, Amer. Meteor. Soc., P8.28, https://ams.confex.com/ams/pdfpapers/175398.pdf.

——, J. G. LaDue, J. T. Ferree, K. Scharfenberg, C. Maier, and W. L. Coulbourne, 2013: Tornado intensity estimation: Past, present, and future. *Bull. Amer. Meteor. Soc.*, **94**, 641–653, https://doi.org/10.1175/BAMS-D-11-00006.1.

——, G. W. Carbin, and S. F. Corfidi, 2015: Overview of the Storm Prediction Center. *13th History Symp.*, Phoenix, AZ, Amer. Meteor. Soc., 1.1, https://ams.confex.com/ams/95Annual/webprogram/Manuscript/Paper266329/sympaper-v3.pdf.

Elsner, J. B., T. H. Jagger, and I. J. Elsner, 2014: Tornado intensity estimated from damage path dimensions. *PLOS ONE*, **9**, e107571, https://doi.org/10.1371/journal.pone.0107571.

——, E. Ryan, and G. Strode, 2018: Structural property losses from tornadoes in Florida. *Wea. Climate Soc.*, **10**, 253–258, https://doi.org/10.1175/WCAS-D-17-0055.1.

——, T. Fricker, and Z. Schroder, 2019: Increasingly powerful tornadoes in the United States. *Geophys. Res. Lett.*, **46**, 392–398, https://doi.org/10.1029/2018GL080819.

Fricker, T., J. B. Elsner, and T. H. Jagger, 2017: Population and energy elasticity of tornado casualties. *Geophys. Res. Lett.*, **44**, 3941–3949, https://doi.org/10.1002/2017GL073093.

Fujita, T. T., 1971: Proposed characterization of tornadoes and hurricanes by area and intensity. University of Chicago SMRP Research Paper 91, 42 pp.

——, 1981: Tornadoes and downbursts in the context of generalized planetary scales. *J. Atmos. Sci.*, **38**, 1511–1534, https://doi.org/10.1175/1520-0469(1981)038<1511:TADITC>2.0.CO;2.

——, 1989: The Teton-Yellowstone tornado of 21 July 1987. *Mon. Wea. Rev.*, **117**, 1913–1940, https://doi.org/10.1175/1520-0493(1989)117<1913:TTYTOJ>2.0.CO;2.

——, 1992: *Memoirs of an Effort to Unlock the Mystery of Severe Storms during the 50 Years, 1942–1992*. University of Chicago Press, 298 pp.

——, 1993: Plainfield tornado of August 28, 1990. *The Tornado: Its Structure, Dynamics, Prediction, and Hazards. Geophys. Monogr.*, Vol. 79, Amer. Geophys. Union, 1–17.

Garner, J. M., W. C. Iwasko, T. D. Jewel, R. L. Thompson, and B. T. Smith, 2021: An environmental study on tornado path-length, longevity, and width. *Wea. Forecasting*, **36**, 1471–1490, https://doi.org/10.1175/WAF-D-20-0230.1.

Gensini, V. A., and H. E. Brooks, 2018: Spatial trends in United States tornado frequency. *npj Climate Atmos. Sci.*, **1**, 38, https://doi.org/10.1038/S41612-018-0048-2.

Grazulis, T. P., 1993: *Significant Tornadoes: 1680–1991: A Chronology and Analysis of Events*. Environmental Films, 1340 pp.

Hales, J. E., Jr., 1988: Improving the watch/warning program through use of significant event data. Preprints, *15th Conf. on Severe Local Storms*, Baltimore, MD, Amer. Meteor. Soc., 165–188.

LaDue, J. G., 2016: About the ASCE Tornado Wind Speed Estimation Standards Committee. *28th Conf. on Severe Local Storms*, Portland, OR, Amer. Meteor. Soc., 6B.1, https://ams.confex.com/ams/28SLS/webprogram/Paper300684.html.

——, and K. Ortega, 2008: Experiences in using the EF-scale since its inception. Preprints, *24th Conf. on Severe Local Storms*, Savannah, GA, Amer. Meteor. Soc., 8B.6, https://ams.confex.com/ams/pdfpapers/142166.pdf.

——, J. Wurman, M. Levitan, F. T. Lombardo, C. D. Karstens, J. Robinson, and W. Coulbourne, 2018: Advances in development of the ASCE/SEI/AMS standard for wind speed estimation in tornadoes and other windstorms. *29th Conf. on Severe Local Storms*, Stowe, VT, Amer. Meteor. Soc., 29, https://ams.confex.com/ams/29SLS/webprogram/Paper348726.html.

Long, J. A., and P. C. Stoy, 2014: Peak tornado activity is occurring earlier in the heart of "Tornado Alley." *Geophys. Res. Lett.*, **41**, 6259–6264, https://doi.org/10.1002/2014GL061385.

——, ——, and T. Gerken, 2018: Tornado seasonality in the southeastern United States. *Wea. Climate Extremes*, **20**, 81–91, https://doi.org/10.1016/j.wace.2018.03.002.

Lu, M., M. Tippett, and U. Lall, 2015: Changes in the seasonality of tornado and favorable genesis conditions in the central United States. *Geophys. Res. Lett.*, **42**, 4224–4231, https://doi.org/10.1002/2015GL063968.

Marshall, T. P., 2002: Tornado damage survey at Moore, Oklahoma. *Wea. Forecasting*, **17**, 582–598, https://doi.org/10.1175/1520-0434(2002)017<0582:TDSAMO>2.0.CO;2.

McDonald, J. R., 2001: T. Theodore Fujita: His contribution to tornado knowledge through damage documentation and the Fujita scale. *Bull. Amer. Meteor. Soc.*, **82**, 63–72, https://doi.org/10.1175/1520-0477(2001)000<0063:TTFHCT>2.3.CO;2.

Minor, J. E., J. R. McDonald, and K. C. Mehta, 1977: The tornado: An engineering-oriented perspective. NOAA Tech. Memo. ERL NSSL-82, 196 pp., NTIS PB-281860/AS.

Molthan, A. L., L. A. Schultz, K. M. McGrath, J. E. Burks, J. P. Camp, K. Angle, and G. J. Jedlovec, 2020: Incorporation and use of Earth remote sensing imagery within the NOAA/NWS damage assessment toolkit. *Bull. Amer. Meteor. Soc.*, **101**, E323–E340, https://doi.org/10.1175/BAMS-D-19-0097.1.

Ryzhkov, A., T. J. Schuur, D. W. Burgess, and D. S. Zrnić, 2005: Polarimetric tornado detection. *J. Appl. Meteor.*, **44**, 557–570, https://doi.org/10.1175/JAM2235.1.

Schaefer, J. T., and R. Edwards, 1999: The SPC tornado/severe thunderstorm database. Preprints, *11th Conf. on Applied Climatology*, Dallas, TX, Amer. Meteor. Soc., 215–220.

Shafer, C. M., and C. A. Doswell III, 2010: A multivariate index for ranking and classifying severe weather outbreaks. *Electron. J. Severe Storms Meteor.*, **5** (1), https://ejssm.org/archives/wp-content/uploads/2021/09/vol5-1.pdf.

Smith, B. T., R. L. Thompson, A. R. Dean, and P. T. Marsh, 2015: Diagnosing the conditional probability of tornado damage rating using environmental and radar attributes. *Wea. Forecasting*, **30**, 914–932, https://doi.org/10.1175/WAF-D-14-00122.1.

——, ——, D. A. Speheger, A. R. Dean, C. D. Karstens, and A. K. Anderson-Frey, 2020a: WSR-88D tornado intensity estimates. Part I: Real-time probabilities of peak tornado wind speeds. *Wea. Forecasting*, **35**, 2479–2492, https://doi.org/10.1175/WAF-D-20-0010.1.

——, ——, ——, ——, ——, and ——, 2020b: WSR-88D tornado intensity estimates. Part II: Real-time applications to tornado warning time scales. *Wea. Forecasting*, **35**, 2493–2506, https://doi.org/10.1175/WAF-D-20-0011.1.

Speheger, D. A., C. A. Doswell III, and G. J. Stumpf, 2002: The tornadoes of 3 May 1999: Event verification in central Oklahoma and related issues. *Wea. Forecasting*, **17**, 362–381, https://doi.org/10.1175/1520-0434(2002)017<0362:TTOMEV>2.0.CO;2.

Strader, S. M., W. S. Ashley, T. J. Pingel, and A. J. Krmenec, 2017: Projected 21st century changes in tornado exposure, risk, and disaster potential. *Climatic Change*, **141**, 301–313, https://doi.org/10.1007/s10584-017-1905-4.

Thom, H. C. S., 1963: Tornado probabilities. *Mon. Wea. Rev.*, **91**, 730–736, https://doi.org/10.1175/1520-0493(1963)091<0730:TP>2.3.CO;2.

Thompson, R. L., and M. D. Vescio, 1998: The destruction potential index—A method for comparing tornado days. Preprints, *19th Conf. on Severe Local Storms*, Minneapolis, MN, Amer. Meteor. Soc., 280–282.

Thorne, P. W., and R. S. Vose, 2010: Reanalysis suitable for characterizing long-term trends. *Bull. Amer. Meteor. Soc.*, **91**, 353–361, https://doi.org/10.1175/2009BAMS2858.1.

Verbout, S. M., H. E. Brooks, L. M. Leslie, and D. M. Schultz, 2006: Evolution of the U.S. tornado database: 1954–2003. *Wea. Forecasting*, **21**, 86–93, https://doi.org/10.1175/WAF910.1.

Wagner, M. R., K. Doe, A. Johnson, Z. Chen, J. Das, and R. S. Cerveny, 2019: Unpiloted aerial systems (UASs) application for tornado damage surveys: Benefits and procedures. *Bull. Amer. Meteor. Soc.*, **100**, 2405–2409, https://doi.org/10.1175/BAMS-D-19-0124.1.

Weiss, S. J., and M. D. Vescio, 1998: Severe local storm climatology 1955–1996: Analysis of reporting trends and implications for NWS operations. Preprints, *18th Conf. on Severe Local Storms*, Minneapolis, MN, Amer. Meteor. Soc., 536–539.

Wilks, D. S., 1995: *Statistical Methods in the Atmospheric Sciences: An Introduction*. Academic Press, 467 pp.

Wind Science and Engineering Center, 2006: A recommendation for an enhanced Fujita scale (EF-scale), revision 2. Texas Tech University Publ., 95 pp., http://www.depts.ttu.edu/nwi/pubs/fscale/efscale.pdf.

Wurman, J., and C. R. Alexander, 2005: The 30 May 1998 Spencer, South Dakota, storm. Part II: Comparison of observed damage and radar-derived winds in the tornadoes. *Mon. Wea. Rev.*, **133**, 97–119, https://doi.org/10.1175/MWR-2856.1.